Indian Journal of Biochemistry & Biophysics
Vol. 62, June 2025, pp. 654-664
DOI: 10.56042/ijbb.v62i6.15237

BMSC-derived exosomes regulate the miR-133b/NLRP3 axis to protect against injury to the spinal cord

Yijia Jia, Tingsheng Lu, Jianwen Yang & Chunshan Luo*
Department of Seven orthopedic wards, Beijing Jishuitan Hospital, Guizhou Hospital, Guiyang-550 014, China

Received 22 November 2024; *revised 20 December 2024*

Spinal cord injury (SCI) can lead to permanent disability in affected patients. Previous studies have indicated that mesenchymal stem cells (MSCs) hold potential as therapeutic tools for treating SCI, but the specific mechanisms underlying their effectiveness have yet to be determined. This study aimed to evaluate the functional significance of exosomes produced from bone marrow mesenchymal stem cells (BMSCs) in treating SCI, explicitly focusing on the regulatory mechanism involving miR-133b and NLRP3. SCI rats received intravenous tail-vein injections of BMSC exosomes (control or miR-133b exosomes). The spinal tissue levels of miR-133b in SCI rats were determined by qPCR. Hind-limb motor function was assessed using Basso Beattie Bresnahan (BBB) scores and Western blot was utilized for analysis of NLRP3 protein levels. Damage and regeneration of spinal neurons were assessed using Nissl, immunofluorescent staining, and immunohistochemistry. Exosomes were successfully harvested from BMSCs following miR-133b transfection, and acute improvements in SCI recovery were observed following the exosomal delivery of miR-133b, as evidenced by short-term improvements in the survival of neurons and associated functional recovery. These miR-133b-containing exosomes were also able to mitigate neuroinflammatory activity by suppressing astrocyte and microglia activation. MiR-133b, at the molecular level, can decrease the production of NLRP3 mRNA by binding to its 3'-untranslated region. As a result, it inhibits the activation of the NLRP3 inflammasome, which is a crucial factor in the neuroinflammatory activity and neuronal damage associated with SCI. The results presented here provide compelling evidence that exosomes isolated from bone marrow-derived microglia overexpressing miR-133b can, at least partially, mitigate the severity of spinal cord injury by targeting the miR-133b/NLRP3 axis in the acute phase. However, due to the short survival time of the subjects, the long-term effects remain unclear, necessitating further investigation of this treatment approach.

Keywords: Bone marrow mesenchymal stem cells (BMSCs), Exosomes, miR-133b, NLRP3 inflammasome, Spinal cord injury (SCI)

Spinal cord injuries (SCIs) are incredibly severe and affected patients often become permanently disabled[1]. Symptoms that can arise following SCI include loss of sensation, reduced motor function, and even paralysis[2]. SCIs are associated with both primary and secondary damage. These mechanisms include the direct physical damage that causes the disorder, as well as related issues such as reduced blood flow, increased oxidative stress, and inflammatory activity[3]. The direct physical damage leads to disruption of axonal integrity and neuronal cell death. Reduced blood flow results in hypoxia and nutrient deprivation, further exacerbating the neuronal damage. Increases in oxidative stress induce peroxidation of lipids and damage to DNA, while increased inflammation leads to activation of astrocytes, microglia, and immune cell infiltration, accompanied by the production of pro-inflammatory factors[4,5]. Despite substantial progress in treating many medical problems, there is still a shortage of effective methods for managing SCI, highlighting the necessity of developing innovative therapeutic techniques.

Researchers have recently identified exosomes, which are small membrane-enclosed vesicles produced by stem cells and most other cells, as potentially effective tools for use in treating SCI[6]. Importantly, exosomes can transport large molecules such as microRNAs (miRNAs), which can be taken up by recipient cells, leading to biological alterations in local or distant cells[7]. In SCI and other neurological diseases, exosomes have been demonstrated to exhibit neuroprotective activity[7-9]. For example, it was determined that exosomes derived from bone marrow mesenchymal stem cells (BMSCs) were able to suppress the activation of astrocytes and to support tissue repair following traumatic SCI[10]. The neuroprotective effects of exosomes may be attributed to their ability to transfer various bioactive molecules,

*Correspondence:
E-mail: jiayijia2192@126.com

such as miRNAs, proteins, and lipids. The transferred miRNAs can regulate gene expression in recipient cells, potentially modulating neuroprotective cellular processes. For instance, miRNAs may target genes related to inflammation, apoptosis, or axonal regeneration, thereby influencing the outcome of SCI. Further research highlighted the ability of exosomes to modulate antioxidant enzyme and cytokine expression levels within damaged spinal cord tissue[11], thus mitigating oxidative and inflammatory stress. Exosomes harvested from BMSCs have further been shown to support axonal regrowth and associated functional improvements following SCI[12]. Further research confirmed that exosomes can enhance the process of myelination and the formation of neurites by transporting growth factors to damaged neurons[13]. These previous findings emphasize the potential usefulness of exosomes for treating SCI. However, the exact methods by which exosomes produced from BMSCs work in this therapeutic environment have yet to be determined.

As small RNAs lack coding activity, miRNAs primarily exert their biological effects by binding target mRNAs through complementary 3'-untranslated region (UTR) sequences. Specific miRNAs have been demonstrated to shape essential processes such as proliferative activity, differentiation, and apoptotic cell death[14]. Several miRNAs have been identified as effective mediators of SCI, making them potential targets for therapeutic intervention. miR-133b has been found to modulate neuronal survival and differentiation[15,16]. The multi-protein NLRP3 inflammasome serves as a central coordinator of many inflammatory and immunological responses[17], with its activation having been tentatively linked to SCI pathophysiology such that inhibiting NLRP3 inflammasome activity offers beneficial efficacy when employed as a treatment for affected patients[18,19]. miR-133b may regulate the NLRP3 inflammasome by binding directly to its 3'-untranslated region, suppressing the production of NLRP3 mRNA and subsequent protein synthesis. This inhibition of the NLRP3 inflammasome can reduce the production of pro-inflammatory factors, such as the cytokine interleukin-1β (IL-1β), and caspase-1 activation, thereby mitigating the neuroinflammatory response and protecting neurons from damage[20]. Additionally, the regulation of NLRP3 by miR-133b may also influence other cellular processes related to SCI, such as autophagy and mitochondrial function.

This study investigated the impact of exosomes produced from BMSCson the development of SCI, with a specific emphasis on the miR-133b/NLRP3 pathway. The experiments were conducted with the assumption that miR-133b would have therapeutic effects on SCI by promoting neuron survival and functional recovery. This would be achieved by suppressing NLRP3, which would, in turn, reduce neuroinflammatory activity. The present investigation finally demonstrated that the use of miR-133b-transfected exosomes obtained from BMSCs effectively reduĴd the expression of NLRP3 and provided protection against SCI. These findings highlight the potential therapeutic utility of utilizing miR-133b-loaded exosomes as a therapy option for patients with SCI.

Materials and Methods

Animals

Male Sprague-Dawley rats (230-250 g, n=40, age=3 months) were obtained from Jiesijie Experimental Animal Company (Shanghai, China).The study was approved by Institutional Review Board (IRB) of the Guizhou Province Osteological Hospital ethics committee in Guiyang, China (Approval number: 20210705).

BMSC Isolation

Femurs and tibiae were harvested from 3-week-old SD rats, after which PBS was used to flush out the bone marrow. The isolated cells were added to DMEM with 10% FBS and 1% penicillin-streptomycin (Gibco, NY, USA), followed by transfer into a 25 cm^2 culture flask for culture in a standard humidified 37°C incubator under 5% CO_2. PBS was employed to wash these cells after 24 h in order to remove any non-adherent cells. Subsequently, the media was replaced every three days. The cells were collected using a solution of 0.25% trypsin-EDTA when they reached 80% confluence, and were re-plated in culture dishes at 1×10^4 cells/cm^2. The identities of isolated BMSCs were confirmed using a FACS can flow cytometer (BD Biosciences). This was performed by staining the cells with antibodies that recognize CD34, CD45, CD44, and CD90 (Invitrogen, CA, USA). Experiments were conducted using BMSCs from passages 3-5.

BMSC transfection and exosome collection

The transfection of BMSCs with miR-133b mimic and negative control constructs was performed using

Lipofectamine 3000 (Invitrogen, USA) in serum-free medium, following the provided protocols from Genechem (Shanghai, China). Media was exchanged after 24 h, followed by culture for a further 48 h. Exosomes were harvested from these cells with an Exo Quick-TC kit (SBI, USA) based on the provided directions. Then, a Libra 120 transmission electron microscope (Zeiss, Germany) was used for ultrastructural examination. In contrast, Western immunoblotting was utilized to analyze the exosomal markers CD9, CD63, and CD81 using antibodies purchased from Abcam (UK).

Rat SCI Model Establishment

Following anesthetization using 1% sodium pentobarbital (50 mg/kg, *i.p.*), the surface skin was disinfected, and a 2-3 cm incision was made in the midline proximal to the T10 spinous process, followed by muscle dissection to expose the vertebrae and extraction of the lamina and spinous processes enabling full exposure of the T10 spinal cord. The NYU/MASCIS modified Allen device (Chinese Academy of Medical Sciences/Peking Union Medical College, Beijing, China) was used (10 g/cm, impact or pestle diameter: 2 mm), dropping the impact or pestle onto the spinal cord from a height of 70 mm. Following that, the incision site was cleansed with a saline solution containing penicillin, then sealed, and the rats were given time to recover. SCI modeling was considered successful if rapid hemostasis in the spinal cord and lower limb tremors were evident in these animals. Sham-operated control rats underwent all the same operative procedures except for the application of the impactor device.

Experimental Grouping

Rats were randomly assigned into four groups (n=10 each), including a sham control group, a SCI model group in which rats were administered PBS, a control exosome treatment group in which rats were administered exosomes from miR-con-transfected BMSCs, and a miR-133b exosome group in which rats were administered exosomes from miR-133b-transfected BMSCs. The exosomes were delivered intravenously through the tail vein (200 μg/mL, 200 μL) one hour after establishing the spinal cord injury model. A total of three injections were provided to each rat, with a one-day interval between each round of injections. Rats were additionally administered penicillin ($2x10^5$ U/kg) daily for three days, with manual expulsion of urine three times daily until the rats had resumed active urination[21]. The experimental progress of this study is shown in (Fig. 1).

Behavioral analysis

Locomotion was evaluated in the rats with Basso-Beattie-Bresnahan (BBB) scores[22]. These scores range from 0 (paralysis) to 21 (normal locomotion). Two

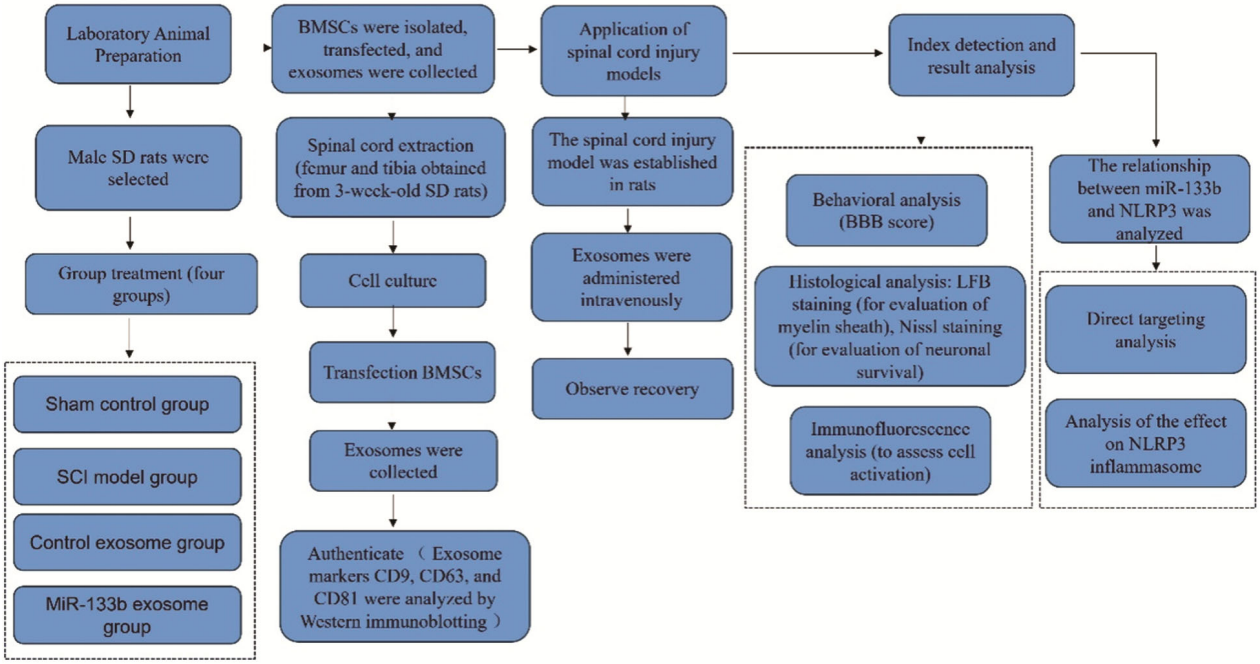

Fig. 1 — Flow diagram of outcome showing the experimental progress

investigators familiar with the assessment procedures and blinded to the groupings independently assessed locomotory function. The scores provided by the investigators were averaged to yield the final score for the individual rats.

Histological analysis

Following the BBB assessment on day 14, the rats were anesthetized and 10 mM segments of the spinal cord including the injury site were removed. Frozen sections (20 μM) were cut with a Superfrost Plus cryomicrotome (Thermo Fisher). White matter was assessed in serial sections cut at 1 mm intervals along the spinal cord. Sections of tissue collected 1-2 mm from the injury epicenter in the caudal and rostral directions were stained with Luxol Fast Blue (LFB) for evaluation of myelination. The sections were evaluated under light microscopy (Olympus, Japan).

Nissl staining

Spinal cord tissues were fixed with 4% methyl alcohol, paraffin-embedded, and cut into sections. The sections were then deparaffinized and treated overnight with a 1:1 mixture of pure ethanol and chloroform at room temperature. This was followed by rehydration by successive immersion in 100% ethanol, 95% ethanol, and dH_2O and staining for 10 min with Tar purple (0.1%, pH=3) at 37°C. The sections were then rinsed with dH_2O, followed by differentiation with 95% ethanol for 5 min, dehydration for 5 min with 100% ethanol and xylene, mounting, and imaging with a microscope (Olympus). Surviving neurons showed blue-stained Nissl bodies and were counted by two blinded investigators within a 500 μM diameter of the injury epicenter. The observers judged whether the surviving neurons after Nissl staining should be counted based on cell morphology (with typical neuronal characteristics such as multipolar shape, obvious cell body, and protrusions), staining characteristics (showing specific Nissl staining in the distribution of dark blue Nissl bodies), cell integrity (excluding obviously damaged or abnormally shaped cells), and location characteristics (within the expected tissue area).

qPCR

The RNA extraction from cells, exosomes, and spinal cord tissue samples was performed using TRIzol (Invitrogen) following the given instructions. Subsequently, cDNA was prepared using the Prime-Script RT kit (TaKaRa, Japan). A miScript SYBR Green PCR kit (QIAGEN, Germany) was then employed to conduct qPCR analyses with appropriate primers (miR-133b, forward, 5′-GCG GCG GAG GTC AGT GC-3′, reverse, 5′-GTG CAG GGT CCG AGG T-3′; U6, forward, 5′-GCT TCG GCA GCA CAT ATA CTA AAA T-3′, reverse, 5′-CGC TTC ACG AAT TTG CGT GTC AT-3′). U6 served as a control for normalization purposes, and the $2^{-\Delta\Delta CT}$ method was used when computing relative RNA levels.

Western immunoblotting

Protein extraction was performed by lysing exosomes, cells, and spinal cord tissues. Protein concentrations were determined with a BCA kit (Beyotime Institute of Biotechnology, Jiangsu, China). After 10% SDS-PAGE protein separation and transfer to nitrocellulose membranes (Millipore, NH, USA), the blots were blocked for 1 h using 5% skim milk followed by incubation with antibodies against CD81 (1:500; Abcam), CD9 (1:500; Abcam), NLRP3 (1:1000; ProteinTech), CD63 (1:500; Abcam), and GAPDH (1:2000; Abcam) at 4°C overnight. The secondary antibody was anti-mouse HRP-conjugated IgG (Promega; w402B, 1:20, 000). Afterward, a protein detection system (ECL, Thermo Fisher) was employed. Band densities were analyzed with ImageJ (NIH, USA), with GAPDH as loading control.

Immunofluorescence

Harvested spinal cord sections were rinsed thrice using PBST (10 min each), blocked (5% goat serum, 1 h), and stained at room temperature with rabbit anti-CD68 or anti-GFAP (both 1:50; Abcam) overnight. After three additional PBS washes, the sections were stained for 1 h using goat anti-rabbit IgG (Invitrogen). They were then counterstained for 2 minutes with DAPI and mounted with non-fluorescent mounting medium (Dako, Glostrup, Denmark). Finally, the sections were evaluated using a confocal laser scanning microscope (Olympus). Five randomly selected fields were analyzed from each section to quantify the number of cells positive for GFAP or CD68.

Immunohistochemical staining

Spinal cord sections prepared as above were rinsed with PBS following deparaffinization, treated for 10 min with boiling citrate buffer (pH 6.0), and then treated using 3% H_2O_2 for 15 min. The sections were then blocked for 1 h using a solution of 10% BSA in

PBS. They were subsequently probed overnight at 4°C with antibodies that specifically target NLRP3, caspase-1, ASC, or IL-1β (at a concentration of 1:500; ProteinTech, Wuhan, China). After rinsing, the sections were probed for an additional 1 hwith HRP goat anti-rabbit IgG. DAB was then used to develop color, followed by hematoxylin counterstaining and light microscope (Olympus) imaging. ImageJ was used for image analysis.

Cell culture and transfection

PC12 cells (ATCC, VA, USA) were grown in complete medium in a standard humidified 37°C incubator under 5% CO_2. Lipofectamine 3000 (Invitrogen) was used to transfect these cells with miR-133b mimic or miR-133b inhibitor constructs or appropriate negative controls (Genepharma, Shanghai, China) based on provided instructions.

Luciferase assays

The TargetScan program was used to detect putative miR-133b binding sites in the 3'-UTR of NLRP3. Wild-type (WT) plasmids were prepared by amplifying and cloning the NLRP3 3'-UTR into the pGL3 luciferase reporter vector (Promega, MWI, USA). At the same time, a Directed Mutagenesis system (Invitrogen) was utilized to generate a mutated (mut) plasmid. After introducing these plasmids along with miR-133b mimic, inhibitor, or control constructs into PC12 cells using Lipofectamine 3000 (Invitrogen), the cells were then cultured for 48 h. Subsequently, the cells were ruptured, and luciferase activity was quantified using a kit (Promega).

Statistical analysis

Statistical testing was performed using GraphPad Prism v7.0 (GraphPad, CA, USA). The results are presented as means ± standard deviation (SD) and were analyzed using t-tests or least significant difference (LSD) ANOVAs. BBB score comparisons were made with Mann-Whitney U tests. $P< 0.05$ was the cut-off used when defining statistical significance.

Results

BMSC-derived exosomal analysis

Flow cytometry was initially used for confirmation of isolated BMSCs from rats by analyzing their CD34, CD44, CD45, and CD90 expression profiles (Fig. 2). As expected, these cells were highly positive for CD44 and CD90, whereas minimal CD34 or CD45 positivity was evident. RNA was harvested from BMSCs at 48 h post-transfection, and qPCR confirmed that miR-133b transfection was associated with higher miR-133b levels in these cells as compared to miR-con-transfected cells (Fig. 3A). Exosomes produced from these two groups of BMSCs were confirmed to be ~100 nm in diameter and to have the anticipated cup-shaped morphological properties by TEM investigations (Fig. 3B). Western immunoblotting further confirmed that these exosomes expressed the expected CD9, CD63, and CD81 surface proteins (Fig. 3C). BMSCs transfected with miR-133b showed markedly increased levels of this miRNA in isolated exosomes when compared to cells transfected with miR-con (Fig. 3D). These findings together verified the effective separation of exosomes originating from BMSCs that are enriched with miR-133b.

Exosomal delivery of miR-133b promotes post-SCI functional recovery

In order to evaluate the efficacy of exosomal miR-133b in reducing damage associated with SCI, a rat model of SCI was created, and these animals were administered the exosomes intravenously, which were produced as described earlier. Initial qPCR analyses confirmed that miR-133b levels at the site of injury were markedly lower in SCI model rats compared with the sham control rats. In contrast, these levels were

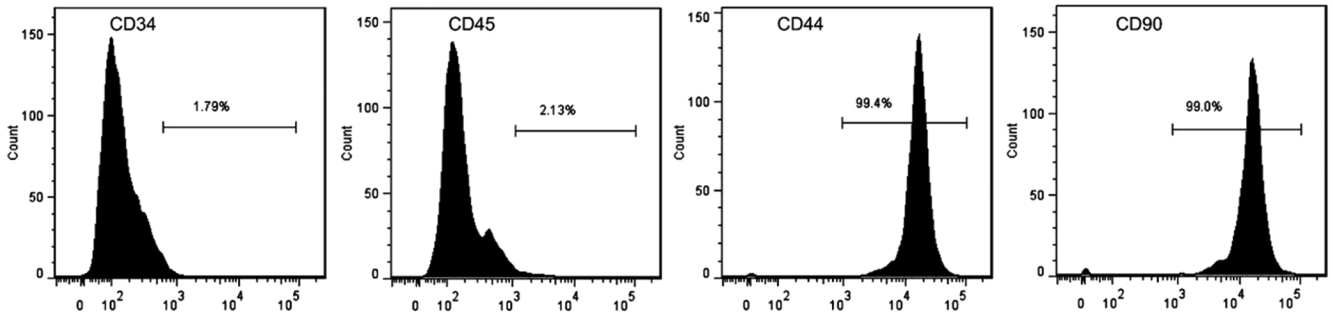

Fig. 2 — BMSC phenotypic verification.CD34, CD44, CD45, and CD90 in rat-derived BMSCs, shown by flow cytometry

markedly higher in rats treated with miR-133b-enriched exosomes relative to all other SCI model groups (Fig. 4A). Hindlimb functional recovery was was monitored using BBB scoring. BBB scores were measured at 1, 3, 7, and 14 days postoperatively, showing no significant differences in scores among the groups at 1 and 3 days after SCI (P>0.05). However, the differences in BBB scores were significantly increased in miR-133b exosome-treated rats on day 7 (#P< 0.05) as well as on day 14 after SCI compared with SCI-treated rats (# #P< 0.01). This demonstrated that the miR-133b exosome group had considerably better functional recovery compared to the other two groups of rats in the SCI model (Fig. 4B).

LFB staining was performed to assess the condition of myelin in the spared white matter, as well as neuronal survival, which is another key factor in motor recovery after SCI. The LFB staining data showed that the miR-133b exosome group significantly reduced myelin loss at 2 mm rostral and caudal of the injury site and at the epicenter (Fig. 5A).

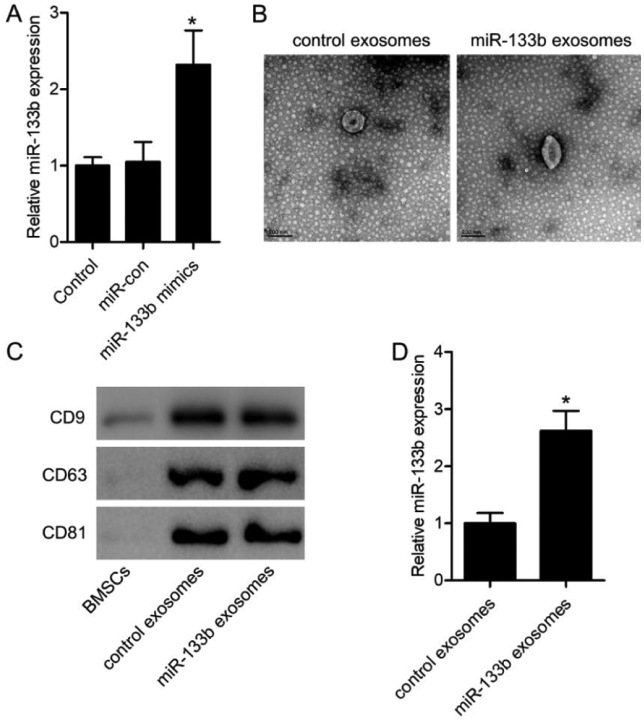

Fig. 3 — Characterization of BMSC-derived exosomes. (A) qPCR was used to assess miR-133b levels in BMSCs following miR-con or miR-133b transfection. *P< 0.05 *vs.* control and miR-con. (B) BMSC-derived exosomes from cells transfected as in (A) were analyzed *via* TEM. Scale bar: 200 nm. (C) Western blots showing levels of exosomal surface proteins (CD9, CD63, and CD81) in BMSC and exosomal samples. (D) miR-133b levels were analyzed *via* qPCR in exosomes from BMSCs transfected as in (A). *P< 0.05 *vs.* control

The spared white matter area was quantified using Image J software. The results showed that the miR-133b exosome group had a significantly larger

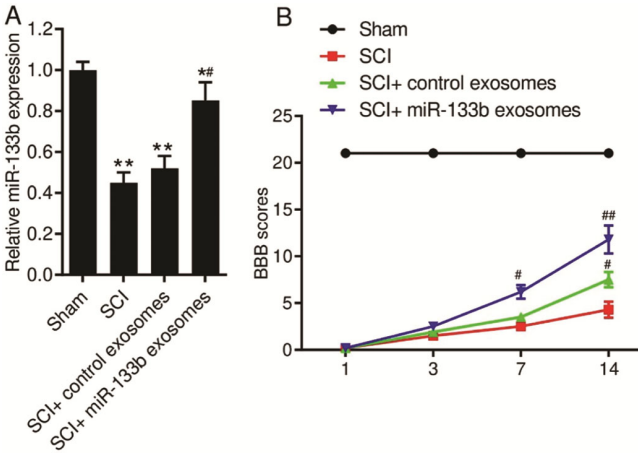

Fig. 4 — Exosome-mediated miR-133b delivery enhances post-SCI functional recovery. (A) miR-133b levels at the injury site following SCI in the indicated treatment groups, assessed by qPCR. (B) Recovery of hindlimb function on days 1, 3, 7, and 14 after SCI shown by the Basso-Beattie-Bresnahan (BBB) scoring system. n=5/group. *P< 0.05, **P< 0.01 *vs.* sham. #P< 0.05, ##P< 0.01 *vs.* SCI

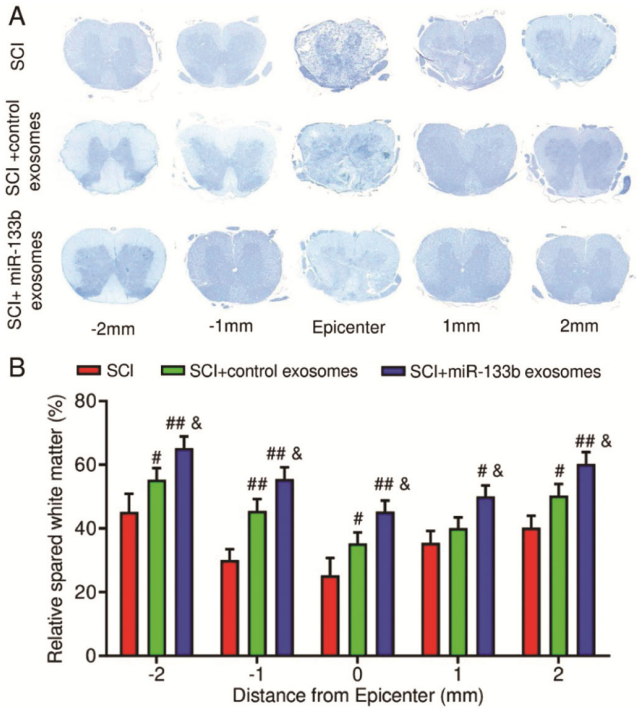

Fig. 5 — miR-133b treatment reduces myelin loss following SCI. (A) Luxol fast blue staining of spinal cord tissues on day 14 following SCI. Transverse cryosections were selected 1 mm, 2 mm rostral and caudal of the injury site and at the epicenter. (B) Myelin quantification at 1 and 2 mm rostral and caudal of the injury site and at the epicenter. n=5/group, #P< 0.05, ##P< 0.01 *vs.* SCI. & P< 0.05 *vs.* control exosomes

area of spared white matter relative to the SCI model and control exosome groups at the injury epicenter, at both 1 mm and 2 mm in the rostral and caudal directions (Fig. 5B).

Nissl staining and subsequent quantitative analysis revealed that in the Sham group, the spinal gray matter contained abundant Nissl bodies, low chromatin contents, and normal neurons with obvious nucleoli. In contrast, neurons in the SCI group exhibited severe damage characterized by vacuolated cytoplasm devoid of Nissl bodies. The control exosome group showed mitigation of this damage to some extent, while in the miR-133b exosome rats, the morphology of the neuronal gray matter was preserved with abundant Nissl bodies seen throughout the cytoplasm (Fig. 6A). The number of Nissl-stained neurons within the 500 μm diameter area was markedly greater in the miR-133b exosome group relative to the control exosome group (Fig. 6B).

miR-133b-enriched exosomes suppress astrocyte and microglia activation

Subsequently, immunofluorescence was utilized to visualize spinal cord sections using markers specific for astrocytes (GFAP) and microglia (CD68). This analysis revealed notably elevated levels of activated microglia and astrocytes in the model rats, shown by greater numbers of CD68-positive (Fig. 7A-B) and GFAP-positive (Fig. 7C-D) cells. When rats were treated with miR-133b-enriched exosomes, however, these changes were reversed, consistent with the ability of exosome-derived miR-133b to suppress neuroinflammatory activity in part *via* suppressing astrocytic and microglial activation.

miR-133b directly targets NLRP3

Initial TargetScan analyses confirmed the presence of a candidate miR-133b interaction site in the 3'-UTR of NLRP3 (Fig. 8A). Consequently, PC12 cells were transfected utilizing miR-133b mimic, inhibitor, or

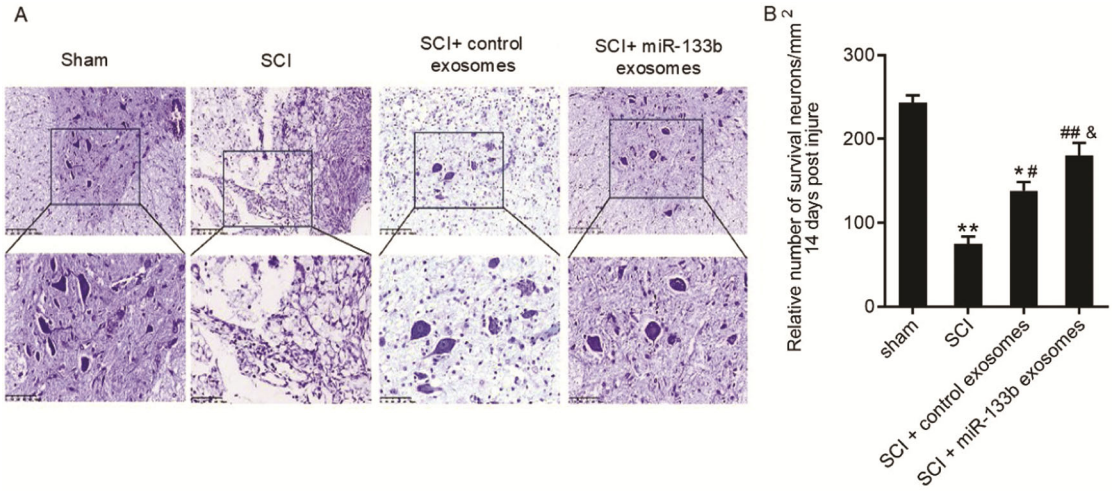

Fig. 6 — miR-133b treatment promotes neuronal survival after SCI. (A) Representative Nissl staining of model and sham rat tissues at 14 day. (B) Quantification of the numbers of Nissl-stained neurons. Scale bar = 100 μm in the above lower-magnification pictures and 50 μm in the below higher-magnification pictures from the boxes of above. n=5/group, * P< 0.05, ** P< 0.01 *vs.* sham. #P< 0.05, ##P< 0.01 *vs.* SCI. & P< 0.05 *vs.* control exosomes

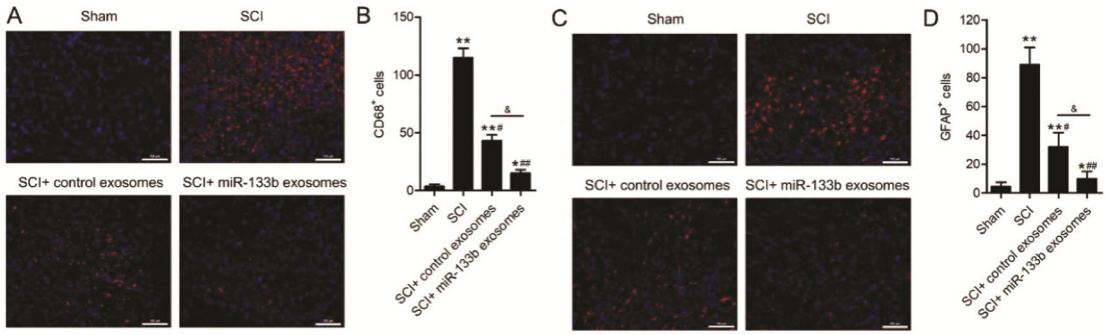

Fig. 7 — The impact of miR-133b-enriched exosomes on astrocytes and microglia. Immunofluorescence showing CD68-positive (A & B) and GFAP-positive (C & D) cells. n=5/group. * P< 0.05, **P< 0.01 *vs.* sham. #P< 0.05, ##P< 0.01 *vs.* SCI. & P< 0.05 *vs.* control exosomes

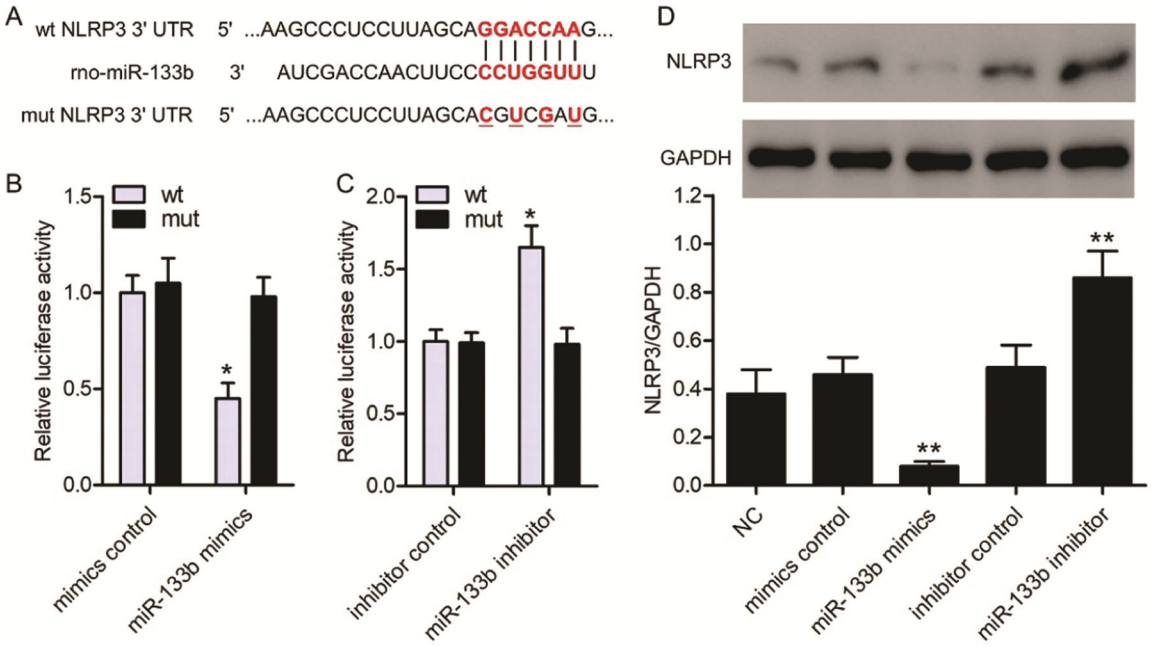

Fig. 8 — miR-133b targets NLRP3. (A) TargetScan prediction of an miR-133b interaction site in WT NLRP3, with the mutated (mut) sequence also being shown. (B & C) A luciferase assay was performed using PC12 cells that had been co-transfected with WT or mut NLRP3 3'-UTR sequences and miR-133b mimics (B) or miR-133b inhibitors (C), together with appropriate negative control constructs. * $P< 0.05$ *vs.* mimic or inhibitor negative controls. (D) NLRP3 levels were detected in PC12 cells following miR-133b mimic, inhibitor, or negative control construct transfection. ** $P< 0.01$ *vs.* NC

negative control constructs and WT or mut NLRP3 3'-UTR reporter plasmids to examine the regulatory function of miR-133b on NLRP3 directly. In comparison to negative control constructions, miR-133b mimics, and inhibitors decreased and increased WT reporter luciferase activity accordingly without affecting the activity of the mutant reporter (Fig. 8B-C). NLRP3 expression was also significantly downregulated in PC12 cells following miR-133b mimic transfection, whereas the opposite effect was observed following miR-133b transfection (Fig. 8D). The data indicated that miR-133b can directly attach to the NLRP3 3′-UTR, hence regulating the expression of this significant pro-inflammatory gene.

Exosome-derived miR-133b inhibits the activation of the NLRP3 Inflammasome

In order to provide a more comprehensive explanation of how exosomal miR-133b affects the activity of the NLRP3 inflammasome associated with SCI, samples of spinal cord tissue were examined using immunohistochemistry labeling for NLRP3, active caspase-1, ASC, and IL-1β. In the SCI model group, the expression of all four of these proteins was increased compared to the samples from sham rats. However, treatment with exosomes enriched with miR-133b dramatically decreased the levels of all four proteins, as shown in (Fig. 9). This reduction is consistent with the inhibition of NLRP3 inflammasome activity.

Discussion

Traumatic spinal cord injury (SCI) is a devastating condition that is often associated with significant loss of function and/or permanent disability[23]. Although the severity of this condition is significant, the available treatment options for these patients are mainly inadequate, highlighting a crucial lack of appropriate medical solutions. Although MSCs have been proposed as prospective therapeutic strategies for treating SCI, the specific processes that explain their effectiveness have yet to be fully understood.

This study investigated the roles of BMSC-derived exosomes as regulators of damage associated with stroke, explicitly focusing on the miR-133b/NLRP3 regulatory pathway. This approach revealed that exosomal miR-133b delivery was sufficient to enhance post-SCI functional recovery in line with prior evidence emphasizing the neuroprotective benefits of this miRNA in SCI and other neurological disorders[24,25]. Exosomes have encouraging benefits over alternative delivery methods, including direct injection or the use of viral vectors, which makes them an excellent choice for the delivery of

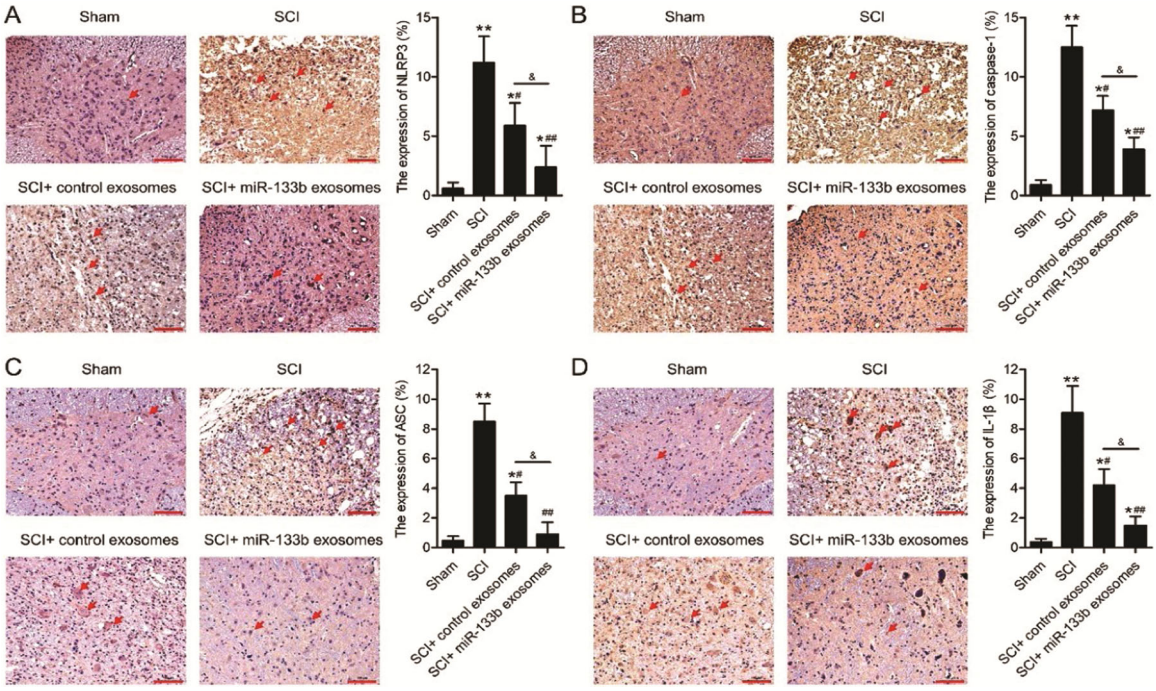

Fig. 9 — The impact of miR-133b-enriched exosomes on the activation of the NLRP3 inflammasome. Immunohistochemical staining of spinal cord tissues from the treatment groups to detect NLRP3 (A), caspase-1 (B), ASC (C), and IL-1β (D). Scale bar: 100 μm. n=5/group. **P*< 0.05, ***P*< 0.01 *vs.* sham. # *P*< 0.05, ## *P*< 0.01 *vs.* SCI. & *P*< 0.05 *vs.* control exosomes

miR-133b[26,27]. Additionally, exosomes are perfect for application in this therapeutic context because they can easily cross the blood-brain barrier and transport miRNAs in a physiological state[28]. The results of BBB score in this study showed that there was no significant difference between the groups at 1 and 3 days after surgery, while at 7 and 14 days after surgery, the scores of the miR-133b exosome group were significantly higher than those of the other SCI model groups, indicating a gradual recovery of motor function. LFB staining showed that the miR-133b exosome group significantly reduced the loss of myelin around the injury site. Nissl staining showed that the neurons in the SCI group were severely damaged, while the morphology of neurons in the miR-133b exosome group was preserved, and there were abundant Nissl bodies in the cytoplasm. The number of Nissl stained neurons was significantly more than that of the control group, reflecting the protective effect on neurons. Here, it was found that miR-133b-enriched exosomes also inhibited the activation of microglia (CD68+) and astrocytes (GFAP+), hence reducing neuroinflammation, which is crucial to the pathophysiology of SCI[29,30]. The immunofluorescence results of the present study showed that the number of activated microglia (CD68+) and astrocytes (GFAP+) was significantly increased in the model rats. Activation of these cells can lead to aggravated neuroinflammation in the pathophysiology of spinal cord injury. However, miR-133b-enriched exosomes inhibit their activation, thereby reducing neuroinflammation and protecting neurons.Using a rat SCI model[31], it was observed that exosomes from human mesenchymal stem cells could alter the microglial response, reduce neuroinflammation, and promote functional recovery. Here, it was observed that the miR-133b exosomes were effective in protecting rats from pathological changes following SCI by enhancing the survival and recovery of neurons, and blocking excessive activation of astrocytes. These findings suggest that miR-133-b exosomes significantly enhanced motor function recovery in the hindlimbs and histological outcomes in SCI rats.

It was discovered that miR-133b directly binds the NLRP3 3'-UTR to inhibit the production of this gene at the molecular level. TargetScan analysis showed that there were miR-133b binding sites in the 3'-UTR of NLRP3. Cell transfection experiments showed that the binding of miR-133b to the 3'-UTR region of NLRP3 could reduce the WT reporter luciferase activity, and down-regulate the expression of NLRP3 in PC12 cells, affecting its gene expression and protein synthesis. This regulation is critical in SCI because NLRP3 plays

a key role in inflammatory activity and its inhibition reduces neuroinflammation and protects neurons. Immunohistochemical staining results showed that the expression of NLRP3, active caspase-1, ASC, and IL-1β was increased in the SCI model group, while miR-133b-enriched exosomes treatment significantly reduced the levels of these proteins, indicating that the activation of NLRP3 inflammasome was inhibited. NLRP3 inflammasome activation is closely related to neuroinflammation after spinal cord injury. Inhibition of NLRP3 inflammasome can reduce neuroinflammation and protect neurons. This is noteworthy since NLRP3 plays a pivotal role in inflammatory activity by activating caspase-1 and producing related inflammatory cytokines[17]. The pathogenesis of SCI and other neurological conditions is believed to be closely related to such NLRP3 inflammasome activity[18,19]. Consequently, our results were in agreement with the capacity of miR-133b-enriched exosomes to prevent NLRP3 inflammasome activation, protecting neurons from SCI-related neuroinflammatory activity and damage.

Conclusion

In conclusion, the current findings demonstrated that BMSC-derived exosomes transfected with miR-133b might inhibit NLRP3 expression, mitigate the severity of SCI by targeting the miR-133b/NLRP3 axis in the acute phase, hence protecting SCI. These findings provide more evidence in favor of using exosome-based therapeutic approaches in the clinic to deliver miR-133b and treat SCI. Nonetheless, there are certain limitations to this study. First of all, the fact that these findings were limited to a rat model system emphasizes the necessity for additional human validation. Secondly, due to the short survival time of the rats in the original study, the long-term effects remain unclear. Further long-term investigations of safety and efficacy outcomes linked with exosomal therapy techniques are necessary. Finally, additional clarification regarding the mechanisms through which miR-133b can modulate functional recovery and neuronal survival will be essential.

Acknowledgement

This study was supported by the Science and Technology Planning Project of Guizhou Province (No. ZK-2022-231) and the High-Level Innovative Talent Initiative of Guizhou Province (No. gzwjrs2024-001).

Conflict of interest

All authors declare no conflict of interest.

References

1 Gillespie ER & Ruitenberg MJ, Neuroinflammation after SCI: Current Insights and Therapeutic Potential of Intravenous Immunoglobulin. *J Neurotrauma,* 39 (2022) 320.

2 Chen G, Wang T, Zhong L, He X, Huang C, Wang Y & Li K, Telemedicine for Preventing and Treating Pressure Injury After Spinal Cord Injury: Systematic Review and Meta-analysis. *J Med Internet Res*, 24 (2022) e37618.

3 Rosales-Antequera C, Viscor G & Araneda OF, Inflammation and Oxidative Stress as Common Mechanisms of Pulmonary, Autonomic and Musculoskeletal Dysfunction after Spinal Cord Injury. *Biology,* 11 (2022).

4 Kirshblum S, Snider B, Eren F & Guest J, Characterizing Natural Recovery after Traumatic Spinal Cord Injury. *J Neurotrauma,* 38 (2021) 1267.

5 Ying Y, Xiang G, Chen M, Ye J, Wu Q, Dou H, Sheng S & Zhu S, Gelatine nanostructured lipid carrier encapsulated FGF15 inhibits autophagy and improves recovery in spinal cord injury. *Cell Death Discov,* 6 (2020) 137.

6 Ge X, Zhou Z, Yang S, Ye W, Wang Z, Wang J, Xiao C, Cui M, Zhou J, Zhu Y, Wang R, Gao Y, Wang H, Tang P, Zhou X, Wang C & Cai W, Exosomal USP13 derived from microvascular endothelial cells regulates immune microenvironment and improves functional recovery after spinal cord injury by stabilizing IκBα. *Cell Biosci,* 13 (2023) 55.

7 Xia X, Wang Y & Zheng JC, Extracellular vesicles, from the pathogenesis to the therapy of neurodegenerative diseases. *Transl Neurodegener,* 11 (2022) 53.

8 Zhou Z, Li C, Bao T, Zhao X, Xiong W, Luo C, Yin G & Fan J, Exosome-Shuttled miR-672-5p from Anti-Inflammatory Microglia Repair Traumatic Spinal Cord Injury by Inhibiting AIM2/ASC/Caspase-1 Signaling Pathway Mediated Neuronal Pyroptosis. *J Neurotrauma,* 39 (2022) 1057.

9 Guo S, Redenski I & Levenberg S, Spinal Cord Repair: From Cells and Tissue Engineering to Extracellular Vesicles.*Cells*, 10 (2021).

10 Zhou Y, Wen LL, Li YF, Wu KM, Duan RR, Yao YB, Jing LJ, Gong Z, Teng JF & Jia YJ. Exosomes derived from bone marrow mesenchymal stem cells protect the injured spinal cord by inhibiting pericyte pyroptosis. *Neural Regen Res*, 17 (2022) 194.

11 Chen J, Wu J, Mu J, Li L, Hu J, Lin H, Cao J & Gao J, An antioxidative sophora exosome-encapsulated hydrogel promotes spinal cord repair by regulating oxidative stress microenvironment. *Nanomedicine*, 47 (2023) 102625.

12 Fan L, Liu C, Chen X, Zheng L, Zou Y, Wen H, Guan P, Lu F, Luo Y, Tan G, Yu P, Chen D, Deng C, Sun Y, Zhou L & Ning C, Exosomes-Loaded Electroconductive Hydrogel Synergistically Promotes Tissue Repair after Spinal Cord Injury *via* Immunoregulation and Enhancement of Myelinated Axon Growth. *Adv Sci (Weinh),* 9 (2022) e2105586.

13 Li S, Liao X, He Y, Chen R, Zheng WV, Tang M, Guo X, Chen J, Hu S & Sun J, Exosomes derived from NGF-overexpressing bone marrow mesenchymal stem cell sheet promote spinal cord injury repair in a mouse model. *Neurochem Int*, 157 (2022) 105339.

14 Mahmoudi E & Cairns MJ, MiR-137: an important player in neural development and neoplastic transformation. *Mol Psychiatry*, 22 (2017) 44.

15 Ren ZW, Zhou JG, Xiong ZK, Zhu FZ & Guo XD, Effect of exosomes derived from MiR-133b-modified ADSCs on the

recovery of neurological function after SCI. *Eur Rev Med Pharmacol Sci*, 23 (2019) 52.

16 Zhou Y, Zhu J, Lv Y, Song C, Ding J, Xiao M, Lu M & Hu G, Kir6.2 Deficiency Promotes Mesencephalic Neural Precursor Cell Differentiation *via* Regulating miR-133b/GDNF in a Parkinson's Disease Mouse Model. *Mol Neurobiol*, 55 (2018) 8550.

17 Jayabalan N, Oronsky B, Cabrales P, Reid T, Caroen S, Johnson AM, Birch NA, O'Sullivan JD & Gordon R, A Review of RRx-001: A Late-Stage Multi-Indication Inhibitor of NLRP3 Activation and Chronic Inflammation. *Drugs*, 83 (2023) 389.

18 Zhang HM, Luo D, Chen R, Wang SH, Zhao YJ, Li JX, Zhou MF, Yu ZM, Zhang JL & Liang FX, Research progress on acupuncture treatment in central nervous system diseases based on NLRP3 inflammasome in animal models. *Front Neurosci*, 17 (2023) 1118508.

19 Mortezaee K, Khanlarkhani N, Beyer C & Zendedel A, Inflammasome: Its role in traumatic brain and spinal cord injury. *J Cell Physiol*, (2018) 5160.

20 Chen Y, Wu L, Shi M, Zeng D, Hu R, Wu X, Han S, He K, Xu H, Shao X & Ma R, Electroacupuncture Inhibits NLRP3 Activation by Regulating CMPK2 After Spinal Cord Injury. *Front Immunol*, 13 (2022) 788556.

21 Li C, Li X, Zhao B & Wang C, Exosomes derived from miR-544-modified mesenchymal stem cells promote recovery after spinal cord injury. *Arch Physiol Biochem*, 126 (2020) 369.

22 .Basso DM, Beattie MS & Bresnahan JC. A sensitive and reliable locomotor rating scale for open field testing in rats. *J Neurotrauma*, 12 (1995) 1.

23 Sterner RC & Sterner RM, Immune response following traumatic spinal cord injury: Pathophysiology and therapies. *Front Immunol*, 13 (2022) 1084101.

24 Shen Y & Cai J, The Importance of Using Exosome-Loaded miRNA for the Treatment of Spinal Cord Injury. *Mol Neurobiol*, 60 (2023) 447.

25 Danilov CA, Thein TZ, Tahara SM, Schönthal AH & Chen TC, Intranasal Delivery of miR133b in a NEO100-Based Formulation Induces a Healing Response in Spinal Cord-Injured Mice. *Cells*, 12 (2023).

26 Liang G, Qin Z, Luo Y, Yin J, Shi Z, Wei R & Ma W, Exosomal microRNA-133b-3p from bone marrow mesenchymal stem cells inhibits angiogenesis and oxidative stress *via* FBN1 repression in diabetic retinopathy. *Gene Ther*, 29 (2022) 710.

27 Wang M, Zhao M, Guo Q, Lou J & Wang L, Non-small cell lung cancer cell-derived exosomal miR-17-5p promotes osteoclast differentiation by targeting PTEN. *Exp Cell Res*, 408 (2021) 112834.

28 Hayashi T & Hoffman MP, Exosomal microRNA communication between tissues during organogenesis. *RNA Biol*, 14 (2017) 1683.

29 Zhang T, Zhang M, Cui S, Liang W, Jia Z, Guo F, Ou W, Wu Y & Zhang S, The core of maintaining neuropathic pain: Crosstalk between glial cells and neurons (neural cell crosstalk at spinal cord). *Brain Behav*, 13 (2023) e2868.

30 Wu Y, Tang Z, Zhang J, Wang Y & Liu S, Restoration of spinal cord injury: From endogenous repairing process to cellular therapy. *Front Cell Neurosci*, 16 (2022) 1077441.

31 Ruppert KA, Nguyen TT, Prabhakara KS, Toledano Furman NE, Srivastava AK, Harting MT, Cox CS & Olson SD, Human Mesenchymal Stromal Cell-Derived Extracellular Vesicles Modify Microglial Response and Improve Clinical Outcomes in Experimental Spinal Cord Injury. *Sci Rep*, 8 (2018) 480.